Structural analyses and material characterisation for the safety assessment of masonry urban infrastructures: implementation of research findings

Esposito, R.; Messali, F.

DOI
10.4233/uuid:3b0d922d-a276-4fb4-bee6-b3412742e10b

Publication date
2023

Document Version
Final published version

Citation (APA)
Esposito, R., & Messali, F. (2023). *Structural analyses and material characterisation for the safety assessment of masonry urban infrastructures: implementation of research findings*. Delft University of Technology. https://doi.org/10.4233/uuid:3b0d922d-a276-4fb4-bee6-b3412742e10b

Important note
To cite this publication, please use the final published version (if applicable).
Please check the document version above.

Project number	C31B20
Report number	C31B20-23-13
Date	September, 05 2023
Version	1

STRUCTURAL ANALYSES AND MATERIAL CHARACTERISATION FOR THE SAFETY ASSESSMENT OF MASONRY URBAN INFRASTRUCTURES: IMPLEMENTATION OF RESEARCH FINDINGS

Project: 2023-2024
Funders: AMS Institute, Municipality of Amsterdam

Editors Rita Esposito
R.Esposito@tudelft.nl
Francesco Messali
F.Messali@tudelft.nl

DOI: 10.4233/uuid:3b0d922d-a276-4fb4-bee6-b3412742e10b

Address Delft University of Technology
Faculty of Civil Engineering and Geosciences
Stevinweg 1, 2628 CN, Delft

How to cite this work
To cite the entire document:
Esposito, R., and Messali, F., *Structural analyses and material characterisation for the safety assessment of masonry urban infrastructures: implementation of research findings*. Report No. CM1B20-13, version 1 (5-9-2023) Delft University of Technology. https://doi.org/10.4233/uuid:3b0d922d-a276-4fb4-bee6-b3412742e10b

To cite a chapter in this document:
Authors' chapter, title's chapter (pp X-X). In Esposito, R and Messali, F. (*Ed*) *Structural analyses and material characterisation for the safety assessment of masonry urban infrastructures: implementation of research findings*. Report No. CM1B20-13, version 1 (5-9-2023) Delft University of Technology.
https://doi.org/10.4233/uuid:3b0d922d-a276-4fb4-bee6-b3412742e10b

Table of Contents

1 Introduction

Since 2022 the engineering office of the municipality of Amsterdam together with AMS institute is funding the TU Delft research programme on "Structural analyses and material characterisation for the safety assessment of masonry city infrastructure". The project is part of the larger programme on bridges an quay walls (PBK). The research is conducted by Dr. M.Eng. Rita Esposito, Dr. M.Eng. Francesco Messali, Dr. M.Eng. Satyadhrik Sharma and M.Eng. Michele Longo from the section of Applied Mechanics in the faculty of Civil Engineering and Geosciences.

The research aims at providing a better understanding of the infrastructure performance, in particular quay walls, to improve the assessment strategy of the municipality within the context of the *Programma Bruggen en Kademuren* (Programme Bridges and Quay walls, *PBK*). Within such programme, the municipality aims at prioritizing the renewal and repair of about 850 traffic bridges and 200 kilometres of quay walls, many of which are located in the historic city centre. To achieve this scope, the Ingenieurs Bureau (IB) Amsterdam has developed a tiered assessment methodology, based on the application of two independent procedures, ARK and TAK. The *Amsterdamse Risicobeoordeling Kademuren* (Amsterdam Risk Assessment of Quay Walls, *ARK*) qualitatively determines the structural condition of a quay wall and identifies critical loading conditions and construction elements. Based on this, either urgent or programmable (safety) measures are prioritized, if necessary, to ensure structural safety. The *Toetskader Amsterdamse Kademuren* (Testing Framework for Amsterdam Quay Walls, *TAK*) aims at predicting quantitatively the remaining lifespan of Amsterdam quay walls, based on the performance of detailed numerical simulations. The TAK is also used in the calibration of the Amsterdam Risk Assessment of Quay Walls (ARK).

This living document collects the main outcomes of the research that can be of use for the municipality, e.g. for improvement of ARK and TAK procedures.

2 Material properties for structural analyses

Author(s): Rita Esposito (r.esposito@tudelft.nl)

2.1 Summary of experimental results

In the project conducted in 2022-2023, an experimental campaign was carried out to characterize shear, compressive and bond properties of samples obtained from a 1.2-m thick bridge's pillar constructed in 1882 in the city of Amsterdam (bridge 41). Both cores and rectangular samples (e.g. prisms, triplets, couplets) were extracted across different locations in the wall thickness to evaluate the effect of exposure to environment conditions. A summary of the material properties obtained is provided in Table 1. A distinction is made between tests and between the wall portion considered. For detailed information please refer to [1].

The following conclusions were drawn:

- Due to the difficulties of extracting rectangular samples from multi-wythe masonry infrastructure, the core testing method seems to be one of the most efficient slightly-destructive test to be employed for characterization of mechanical properties. Additionally, this gives the advantage that in case of composite structures, i.e. masonry-concrete walls or presence of renovation, the same sample can be adopted independently of the construction material.
- For this case study, a through-thickness effect for some compressive properties (elastic modulus and strain at peak) and for the bond properties (flexural bond strength and bond fracture energy) could be identified: the compressive behaviour of the masonry is stiffer and the flexural bond properties are weaker when being closer to water. However, it was not possible to identify a clear trend for the shear properties due to the limited data with a high coefficient of variation.
- Further improvement to the core testing method to assess the mechanical properties of multi-wythe masonry is required. The following aspects are identified for the compressive tests: the study of specimen size and bond pattern on the compressive behaviour, the identification of a better capping material for the estimation of both pre- and post-peak behaviour. The following aspects are identified for the splitting tests on core: prevention of failure in the brick in the case of high bond properties by means of local strengthening of the brick or variation of specimen size.

Table 2 shows a comparison between the obtained results and the results obtained for other Dutch city infrastructures. In particular the following study are considered:

- The experimental campaign performed by TU/e in 2021 concerning bridge 108 in the city of Amsterdam [2]. This bridge was built roughly in the same period of bridge 41.
- The experimental tests performed by TU Delft in 2023 concerning a quay wall structure in an harbour [3]. This quay wall had different construction and renovation phases. The tests were performed on specimens extracted from the part built before 1400 and renovated in 1600.

For the cases considered, the masonry is composed of clay bricks. Detailed investigations on the type of mortar are not present. In reference [2], the presence of cement mortar is mentioned, but no reference to test results is reported.

From the comparison, it is possible to conclude that the average result and the coefficient of variation are generally in the same range. This should be however considered with care since for each type of test, a limited amount of test data is available.

Table 1 – Overview of material properties tested during the project 2022-2023 (Specimen extracted only above water level. Through thickness effect studied: Piece P1-P2-P5 external, Piece P3-P4 internal).

Type test	Properties	Symbol	Unit	Wall piece	Average	C.o.V.	No. test data
Compression test on brick	Normalised compressive strength	f_b	MPa	P2 (ext)	26.71	28%	3
	Normalised compressive strength	f_b	MPa	P4 (int)	26.78	16%	3
Double punch test on mortar	Compressive strength	f_m	MPa	P1-P5	7.61	13%	7
Compression test masonry on T-shape single-wythe core	Elastic modulus	E_{core}	MPa	P1 (ext)	5917	21%	5
	Compressive strength	$f'_{m,core}$	MPa		12.85	17%	5
	Strain at peak	$\varepsilon_{p,core}$	‰		5.5	44%	5
	Compressive fracture energy	$G_{f\text{-}c,core}$	N/mm		19.89	33%	5
	Elastic modulus	E_{core}	MPa	P2 (ext)	5607.7	33%	4
	Compressive strength	$f'_{m,core}$	MPa		11.71	13%	4
	Strain at peak	$\varepsilon_{p,core}$	‰		4.79	45%	4
	Compressive fracture energy	$G_{f\text{-}c,core}$	N/mm		16.53	12%	4
	Elastic modulus	E_{core}	MPa	P3 (int)	2726.2	33%	5
	Compressive strength	$f'_{m,core}$	MPa		12.52	14%	5
	Strain at peak	$\varepsilon_{p,core}$	‰		14.1	43%	5
	Compressive fracture energy	$G_{f\text{-}c,core}$	N/mm		21.15	33%	5
	Elastic modulus	E_{core}	MPa	P4 (int)	3505	7%	2
	Compressive strength	$f'_{m,core}$	MPa		13.09	23%	2
	Strain at peak	$\varepsilon_{p,core}$	‰		10.37	9%	2
	Compressive fracture energy	$G_{f\text{-}c,core}$	N/mm		20.02	23%	2
Compression test masonry on R-shape single-wythe core	Elastic modulus	E_{core}	MPa	P1 (ext)	7279.4	32%	3
	Compressive strength	$f'_{m,core}$	MPa		12.71	9%	3
	Strain at peak	$\varepsilon_{p,core}$	‰		4.37	31%	3
	Compressive fracture energy	$G_{f\text{-}c,core}$	N/mm		10.3	37%	3

Table 1 – Overview of material properties tested during the project 2022-2023 (Specimen extracted only above water level. Through thickness effect studied: Piece P1-P2-P5 external, Piece P3-P4 internal). - continued

Type test	Properties	Symbol	Unit	Wall piece	Average	C.o.V.	No. test data
Compression test masonry R-shape single-wythe core	Elastic modulus	E_{core}	MPa	P2 (ext)	4427.7	14%	2
	Compressive strength	$f'_{m,core}$	MPa		14.02	26%	2
	Strain at peak	$\varepsilon_{p,core}$	‰		5.62	4%	2
	Compressive fracture energy	$G_{f\text{-}c,core}$	N/mm		24.29	41%	2
	Elastic modulus	E_{core}	MPa	P3 (int)	3143.65	22%	2
	Compressive strength	$f'_{m,core}$	MPa		13.35	31%	2
	Strain at peak	$\varepsilon_{p,core}$	‰		6.93	51%	2
	Compressive fracture energy	$G_{f\text{-}c,core}$	N/mm		18.73	58%	2
Compression test masonry R-shape double-wythe core	Elastic modulus	E_{core}	MPa	P3 (int)	1923.6	30%	5
	Compressive strength	$f'_{m,core}$	MPa		12.52	16%	5
	Strain at peak	$\varepsilon_{p,core}$	‰		12.21	34%	4
	Compressive fracture energy	$G_{f\text{-}c,core}$	N/mm		30.6	32%	4
Compression test masonry on H-shape double-wythe core	Elastic modulus	E_{core}	MPa	P3 (int)	2709.12	39%	4
	Compressive strength	$f'_{m,core}$	MPa		11.54	21%	4
	Strain at peak	$\varepsilon_{p,core}$	‰		12.19	43%	3
	Compressive fracture energy	$G_{f\text{-}c,core}$	N/mm		30.88	41%	3
Compression test masonry prisms - H/L = 4brick/1brick	Elastic modulus	E	MPa	P4 (int)	3186.3	20%	3
	Compressive strength	f'_m	MPa		6.89	8%	3
	Strain at peak	ε_p	‰		4.26	13%	2
	Compressive fracture energy	$G_{f\text{-}c}$	N/mm		19.1	47%	2
	Elastic modulus	E	MPa	P5 (ext)	4167.85	19%	4
	Compressive strength	f'_m	MPa		7.45	17%	4
	Strain at peak	ε_p	‰		3.08	47%	2
	Compressive fracture energy	$G_{f\text{-}c}$	N/mm		31.04	62%	2

Table 1 – Overview of material properties tested during the project 2022-2023 (Specimen extracted only above water level. Through thickness effect studied: Piece P1-P2-P5 external, Piece P3-P4 internal). - continued

Type test	Properties	Symbol	Unit	Wall piece	Average	C.o.V.	No. test data
Compression test masonry prisms - H/L = 6brick/1brick	Elastic modulus	E	MPa	P4 (int)	4349	4%	4
	Compressive strength	f'_m	MPa		7.53	13%	4
	Strain at peak	ε_p	‰		3.9	27%	3
	Compressive fracture energy	G_{f-c}	N/mm		17.05	30%	3
	Elastic modulus	E	MPa	P5 (ext)	5757.48	16%	4
	Compressive strength	f'_m	MPa		8.32	11%	4
	Strain at peak	ε_p	‰		4.2	22%	4
	Compressive fracture energy	G_{f-c}	N/mm		27.74	29%	4
Splitting test on I-shaped core	Initial shear strength	f_{v0}	MPa	P1-P4	0.51		18
	Friction coefficient	μ	-		0.83		18
	Mode-II fracture energy	G_{f-II}	N/mm				
Splitting test on I-shaped core	Initial shear strength	f_{v0}	MPa	P4 (int)	0.38		8
	Friction coefficient	μ	-		0.90		8
	Mode-II fracture energy	G_{f-II}	N/mm				
Shear-compression test on triplet	Initial shear strength	f_{v0}	MPa	P2 (ext)	0.32		5
	Friction coefficient	μ	-		0.83		5
	Residual friction coefficient	μ_{res}	-		0.87		
	Mode-II fracture energy	G_{f-II}	N/mm		0.1		3
Bond wrench test	Flexural bond strength	f_w	MPa	P2 (ext)	0.42	5%	3
	Flexural fracture energy	G_{f-w}	N/mm		0.05	0.2%	3
	Flexural bond strength	f_w	MPa	P4 (int)	0.75	13%	3
	Flexural fracture energy	G_{f-w}	N/mm		0.15	35%	3

Table 2 – Comparison of material properties of masonry obtained by various testing campaign on Dutch city infrastructure.

		Structure type, City		Bridge 41, Amsterdam				Bridge 108, Amsterdam			Quay wall harbour			
		Year of construction		1882				1880			before 1400 and 1600			
		Type of brick / Type of mortar		solid clay / NA				solid clay / cement			solid clay / NA			
		Annotations		Specimen extracted only above water level. Through thickness effect studied: Piece P1-P2-P5 external, Piece P3-P4 internal				Specimens extracted in internal part of the wall. Not clear if above and/or below water level.			Specimen extracted above water level and in the first 400 mm of the wall thickness.			
		Tested by / Reference		TU Delft / [1]				TU/e / [2]			TU Delft / [3]			
Type test	**Properties**	**Symbol**	**Unit**	**Location**	**Avg.**	**C.o.V.**	**No. data**	**Avg.**	**C.o.V.**	**No. data**	**Location**	**Avg.**	**C.o.V.**	**No. data**
Compression test on bricks	Normalised compressive strength	f_b	MPa	P2 (ext)	26.71	28%	3	25.47	32%	9				
	Normalised compressive strength	f_b	MPa	P4 (int)	26.78	16%	3							
Compression test masonry on T-shape single-wythe core	Elastic modulus	E_{core}	MPa	P1 (ext)	5917	21%	5				Ext	3113	32%	5
	Compressive strength	$f'_{m,core}$	MPa		12.85	17%	5					10.98	21%	4
	Elastic modulus	E_{core}	MPa	P2 (ext)	5607.7	33%	4							
	Compressive strength	$f'_{m,core}$	MPa		11.71	13%	4							
	Elastic modulus	E_{core}	MPa	P3 (int)	2726.2	33%	5							
	Compressive strength	$f'_{m,core}$	MPa		12.52	14%	5							
	Elastic modulus	E_{core}	MPa	P4 (int)	3505	7%	2							
	Compressive strength	$f'_{m,core}$	MPa		13.09	23%	2							
Compression test masonry specimen with 6 layers	Elastic modulus	E	MPa	P4 (int)	4349	4%	4	4200		4				
	Compressive strength	f'_m	MPa		7.53	13%	4	12.89	21%	5				
Shear-compression test on triplet	Initial shear strength	f_{v0}	MPa	P2 (ext)	0.32		5	0.33		18				
	Friction coefficient	μ	-		0.83		5	1.3		18				
	Residual friction coefficient	μ_{res}	-		0.87			0.85		18				

2.2 Comparison with value prescribed by standards

The mechanical properties obtained in the experimental campaign 2022-2023 are here compared with value prescribed by standards. The following data are considered for information:

- Table F.2 in standard NPR 9998:2020 for the Assessment of structural safety of buildings in case of erection, reconstruction, and disapproval - Induced earthquakes - Basis of design, actions and resistances [4].
- Table 2, 3 and 4 in standard NPR 9096-1-1 Dutch annex to Eurocode 6 [5].

The comparison is made considering the following aspects:

- The comparison is made in terms of mean values.
- For the experimental results, a distinction based on the location (external and internal) is made only for the elastic modulus and the flexural/tensile properties. Weighted average values are calculated considering the different number of test data per location.
- Considering that NPR 9096-1-1 prescribes only characteristics values, the correlation factors in Table 3 are used. These are based on the corresponding testing standard.
- As per the NPR 9998, specific input for nonlinear finite element analyses are derived for the other cases making use of the correlation functions in Table 4.

Table 5 shows comparison between experimental results from project 2022-2023, standard NPR 9998, and Dutch annex to Eurocode 6 (NPR 9096-1-1). The following conclusions can be drawn:

- Compressive strength: value provided by both the standards are slightly conservative with respect to experimental results. The closest estimate is provided by NPR 9998 for clay brick masonry built after 1945
- Elastic and shear modulus: the value provided by the standards are comparable with the experimental results for the external portion of masonry, while they are approximately 50% higher with respect to the results for the internal portion of masonry.
- Flexural tensile strength, uniaxial tensile strength, and fracture energy in tension: their lower value (external portion) is generally higher than the values prescribed by standards.
- Initial shear strength: the experimental value is comparable with the one prescribed by NPR 9998 for clay brick masonry built before 1945.
- Friction coefficient: it is approximately 10% higher than the value prescribed by the NPR 9998 for both clay masonry typologies.
- Compressive fracture energy: the lowest experimental values (internal portion) is in between the values prescribed by the NPR 9998 for the two clay masonry typologies.
- Fracture energy in shear: the experimental value is comparable to the one prescribed by the NPR 9998 for clay brick masonry built before 1945.

Overall, none of the standards prescribes a set of value that is always conservative with respect to the experimental ones. The best compromise would be to consider values provided by NPR 9998 for clay brick masonry built before 1945 with a reduction of 25% in compressive fracture energy; a possible increase in flexural/uniaxial tensile strength may be considered.
Nevertheless, a larger database of mechanical properties for different structural and material typologies is required to further confirm this conclusion.

Table 3 – Correlation factors between mean and characteristic values of mechanical properties of masonry.

Properties	**Ratio between mean and characteristic values**	**Standard testing method**
Compressive strength	1.2	EN 1052-1
Flexural tensile strength for plane of failure parallel to the bed joints	1.3	EN 1052-2
Flexural tensile strength for plane of failure perpendicular to the bed joints	1.3	EN 1052-2
Initial shear strength	1.3	EN 1052-3

Table 4 – Correlation functions for derived material properties.

Properties	**Equation**	**Reference**
Flexural tensile strength for plane of failure parallel to the bed joints as flexural bond strength	$f_{x1} = f_{w1}$	Jafari et al. 2022 [6]
Uniaxial tensile strength (f_{t1}, f_{t2}) as function of flexural tensile strength (f_{x1}, f_{x2})	$f_{t1} = \frac{2}{3} f_{x1}$ $f_{t2} = \frac{2}{3} f_{x2}$	Jafari et al. 2022 [6]
Fracture energy in tension for plane of failure parallel to the bed joints as function of bond fracture energy (bond wrench test)	$G_{t1} = 0.25 G_w$	Gaggero and Esposito 2023 [7]
Elastic modulus as function of characteristic compressive strength of masonry	$E = 700 f_k$	Eurocode 6 [8]
Shear modulus as function of elastic modulus	$G = 0.4E$	Jafari et al. 2021 [6]

Table 5 – Comparison between experimental results from project 2022-2023, standard NPR 9998, and Dutch annex to Eurocode 6 (NPR 9096-1-1) in terms of mean values.

			Amsterdam Bridge 41		**NPR 9998**		**NPR 9096-1-1**
Properties of masonry or brick-mortar interface	**Symbol**	**Unit**	**External**	**Internal**	**Clay brick masonry pre 1945**	**Clay brick masonry post 1945**	**Clay brick**
Compressive strength	f'_m	MPa	12.5[a]		8.5	10	8.72
Elastic modulus	E	MPa	5780[a]	2949[a]	5000	6000	5089
Shear modulus	G	MPa	2312	1179	2000	2500	2036
Flexural tensile strength for plane of failure parallel to the bed joints	f_{x1}	MPa	0.42	0.75	0.15	0.3	0.30[b]
Flexural tensile strength for plane of failure perpendicular to the bed joints	f_{x2}	MPa	-	-	0.55	0.85	1.08[b]
Uniaxial tensile strength for plane of failure parallel to the bed joints	f_{t1}	MPa	0.28	0.50	0.1	0.2	0.20
Uniaxial tensile strength for plane of failure perpendicular to the bed joints	f_{t2}	MPa	-	-	0.35	0.55	0.72
Initial shear strength (bed joints)	f_{v0}	MPa	0.32		0.3	0.4	0.39[b]
Shear friction coefficient (bed joints)	μ		0.83		0.75	0.75	-
Fracture energy in tension for plane of failure parallel to the bed joints[c]	G_{f1}	J/m^2	12.5	37.5	10	10	-
Fracture energy in tension for plane of failure perpendicular to the bed joints[c]	G_{f2}	J/m^2	-	-	35	35	-
Fracture energy in compression[d]	G_{f-c}	J/m^2	27740[e]	17050[e]	20000	15000	-
Fracture energy in shear (bed joints)[c,f]	G_{f-II}	J/m^2	100		100	200	-

[a] From compression tests on T-shape single-wythe core (weighted average considered).
[b] Minimum value for masonry in environment classes other than MX1 and MX2.
[c] The parameter depends on the element mesh. To be used in combination with a crack band width, in case of smeared finite element models.
[d] The parameter depends on the element mesh. To be used in combination with a crush band width, in case of smeared finite element models.
[e] Determined from tests on prisms with six layers (results of core testing are considered not reliable, because show extensive failure of the capping)
[f] Evaluated at the lowest pre-compression level (0.2 MPa)

3 Structural assessment of masonry quay walls by means of numerical simulations

Author(s): Francesco Messali (F.Messali@tudelft.nl), Satyadhrik Sharma (S.Sharma-9@tudelft.nl), Michele Longo (M.Longo@tudelft.nl)

3.1 Summary

In the project conducted in 2022-2023, tailor-made analyses procedures were developed to numerically assess the response of masonry quay walls under the effect of traffic loads. Simulations performed using these analyses procedures included both physical and geometrical non-linearities. These procedures can be adopted to model loading from the passage of vehicles next to the quays in static as well as dynamic conditions, allowing for realistic estimates of structural safety, peak force capacity, and peak/residual displacements. Different contributions to the load redistribution capacity of masonry quay walls were identified due to:

1) time- and space-variance of the applied traffic loading;
2) three-dimensional numerical models, and
3) non-linear material behaviour.

Among these contributions, the performed investigations highlighted that the load redistribution capacity of quay walls due to the consideration of a three-dimensional numerical model as compared to a two-dimensional numerical model is particularly important in the case of quays with damaged foundations. The analysis procedures also exhibited the potential of predicting the failure of the structural components and capturing the effect of foundation damage on the structural response of quay walls under traffic loads. As the developed analysis procedures have not been validated and have only been applied to a single case study, the quantifiable results obtained from the demonstrated application of the analysis procedure, as provided in the [9], cannot be directly used for the structural assessment of all quays. However, several recommendations for the improvement of ARK version 2.0 have been identified based on these simulations:

A. Visible cracks may underestimate the actual crack width under traffic loading
B. Collapse may initiate after the opening of cracks of limited width
C. Displacement and deformation rate limits should be normalized with respect to the geometry of the wall
D. The spatial distribution of foundation damage is a relevant parameter
E. Threshold values for crack width should vary depending on the failure mechanism

The background of such recommendations is summarized in section 3.2.

3.2 Recommendations for future development of ARK based on the analyses performed in project 2022-23

A. Visible cracks may underestimate the actual crack width under traffic loading

In all simulations performed in the project conducted in 2022-2023 [9], the failure mechanism exhibited by the masonry is the local overturning of a section of the quay wall. Due to the kinematics of this mechanism, at its initial stages of development, cracks only become visible on the soil-facing side of the quay wall. Even when the mechanism is fully developed, crack widths (*Scheurwijdte*) remain wider on the soil-facing side of the quay wall compared to the water-facing side (Figure 1). Moreover, crack widths at the time of inspection

might be significantly lower than the crack widths that temporarily open at the passage of a vehicle next to the wall, as cracks tend to close when the quay is unloaded from vehicular traffic (Figure 2). These considerations should be taken into account, especially since it's uncertain whether crack widths are presently inspected solely on the more accessible water-facing side of the quay and during periods of no vehicular traffic on the backfill of quays.

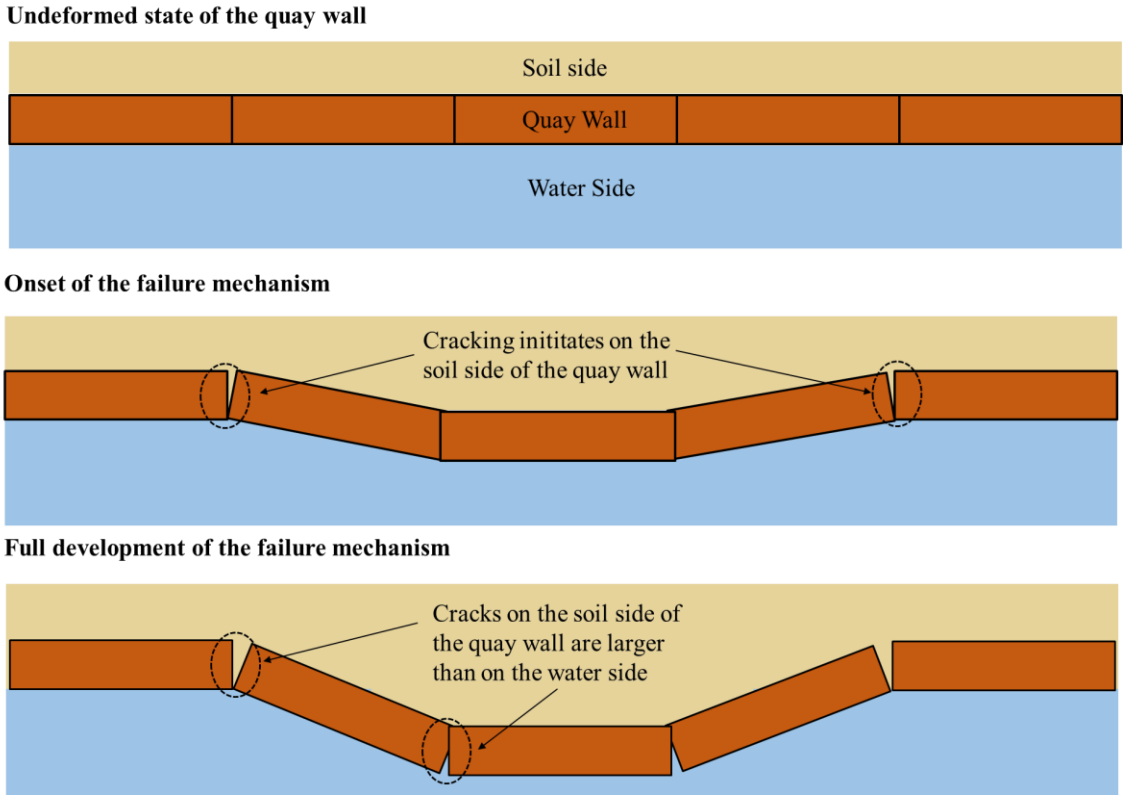

Figure 1: Kinematics of failure mechanism of the quay wall observed from numerical simulations in [9].

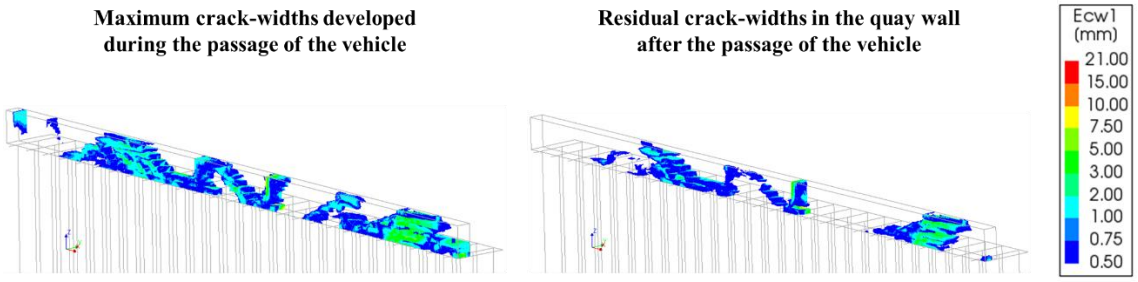

Figure 2: Maximum and residual crack widths in the quay wall during and after the passage of the same vehicle (x10 times design load) from a simulation in [9].

B. Collapse may initiate after the opening of cracks of limited width

The basis of the limits utilized to correlate crack width (*Scheurwijdte*) with the probability of failure (*kans op vallen*) of the quay in ARK 2.0 is not clear. Nonetheless, these limits are very similar to those specified in [10]. It should be noted that such limits were initially intended for application in cases involving buildings erected on shallow foundations and subject to settlement due to excavation. The limits reported in [10] are also

defined on the basis of ease of repairing them rather than being associated with structural damage. The outcomes of the simulations detailed performed in project 2022-2023 [9] suggest that these values might be lower than the thresholds currently employed in ARK 2.0 (Figure 3).

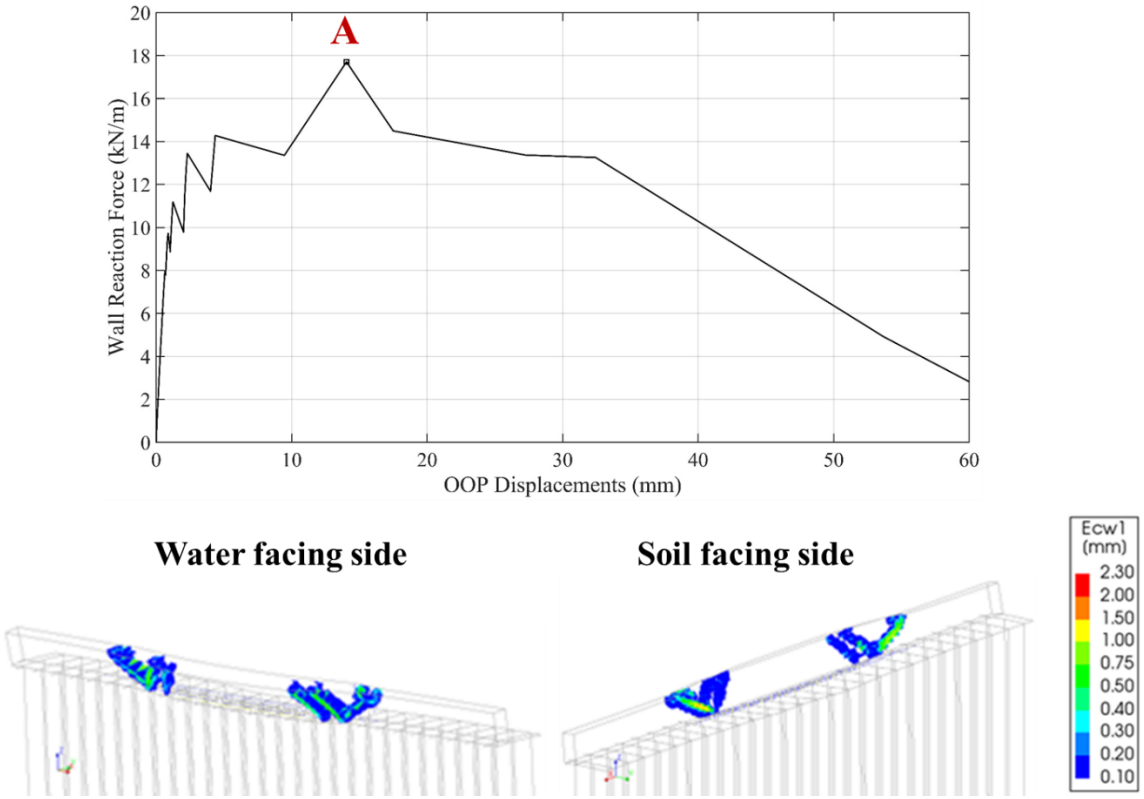

Figure 3: Crack widths in the quay wall at imminent collapse i.e. performance point A of the force-displacement curve from a non-linear static (pushover) analysis reported in [9].

C. Displacement and deformation rate limits should be normalized with respect to the geometry of the wall

In ARK 2.0, the limits for tilting, deformation, and deformation rates of the quay (*Scheefstand in wand, Deformatiewaarde, Deformatiesnelheid*) correlated to the probability of failure (*kans op vallen*) are expressed as displacements (or deformation rates) and do not consider the geometry of the wall. This is counterintuitive, as an out-of-plane deformation of, say, 45 mm, which corresponds to a very high probability of failure (*zeer grote kans op vallen*) for all quay walls in ARK 2.0, could be expected to have significantly different on the structural stability of a 0.55 m thick quay wall as compared to a 1.45 m thick wall. Considering the wide range of geometries of quay walls, it is advisable to normalize these limits to account for the relevant dimensions of the quay.

D. The spatial distribution of foundation damage is a relevant parameter

Numerical simulations carried out in project 2022-2023 [9] highlighted the significant impact of the spatial distribution of foundation damage on the structural capacity of the quay. The presence of the same quantity of non-functional piles within a quay resulted in its collapse under the applied parking load when they were assumed to be positioned adjacent to one another. However, when they were randomly dispersed along its length, the quay could withstand a load ten times greater than the intended design traffic load (Figure 4,

Figure 5). However, in ARK 2.0, probability of failure (*kans op vallen*) of the quay is correlated only to the number of non-functional piles (*Totaal aantal slecht*) among the sampled piles (*Aantal bemonsterde palen*), making no consideration for the locations from where they were sampled from along the quay.

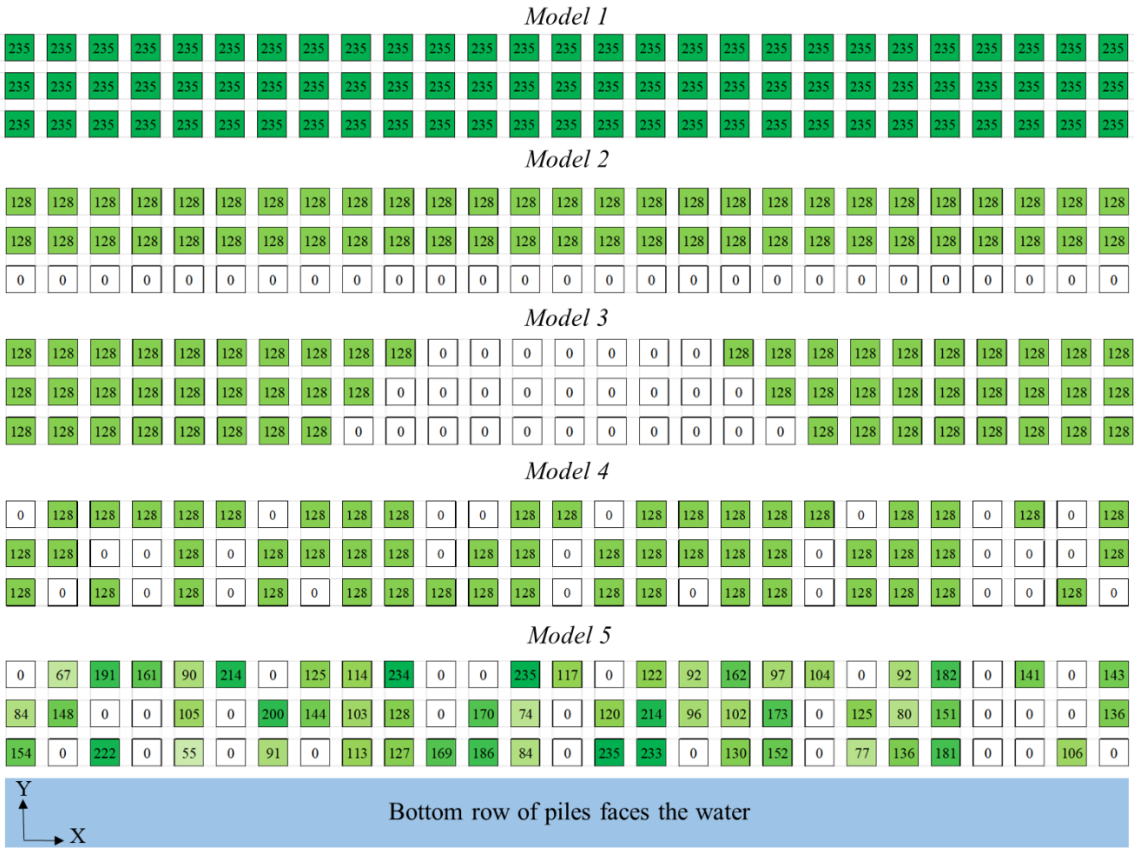

Figure 4: Pile cap diameters in mm assumed for four different numerical models (*Models 2-5*) all considering 27 non-functional piles i.e. piles with 0 mm cap diameter but distributed differently along the length of the quay [9].

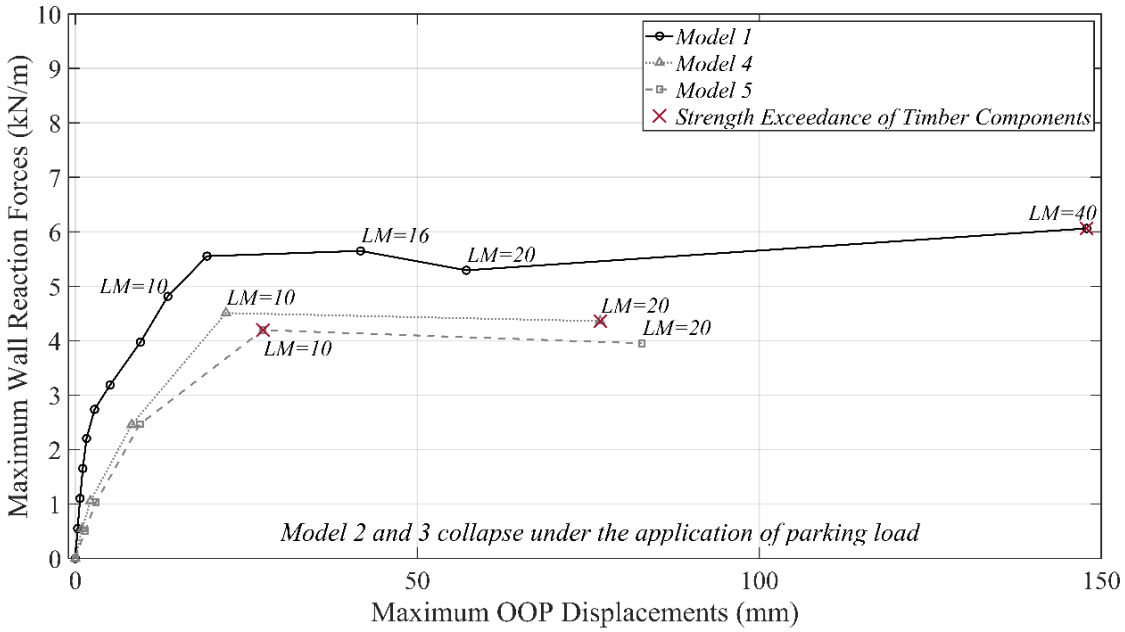

Figure 5: Wall structural capacity reported as force-displacement curves of numerical models (see Figure 3) considering different spatial distribution of 27 non-functional piles [9].

E. Threshold values for crack width should vary depending on the failure mechanism

In general, shape and position of cracks in quay walls depend on the action that cause the cracks. This was also observed in the numerical simulations performed in project 2022-23 [9] (Figure 6). For this reason, the same crack width does not necessarily correspond to the same probability of failure (*kans op falen*) in case of different failure mechanisms, especially when only visible cracks are considered. However, ARK 2.0 makes no distinction for the nature of the cracks observed in the quay wall while calculating its contribution towards the probability of failure. Future developments of ARK should try to account for different contributions to the probability of failure based on the nature of the damage (orientation and position, also in relation to other cracks or to the detected foundation damage). This more complex evaluation can take the form of a diagnostic decision-support tool for assessing structural damage in masonry, as reported in [11], but still requires adequate understanding of the correlation between the failure mechanism, the orientation and position of the cracks and threshold values beyond which collapse is expected.

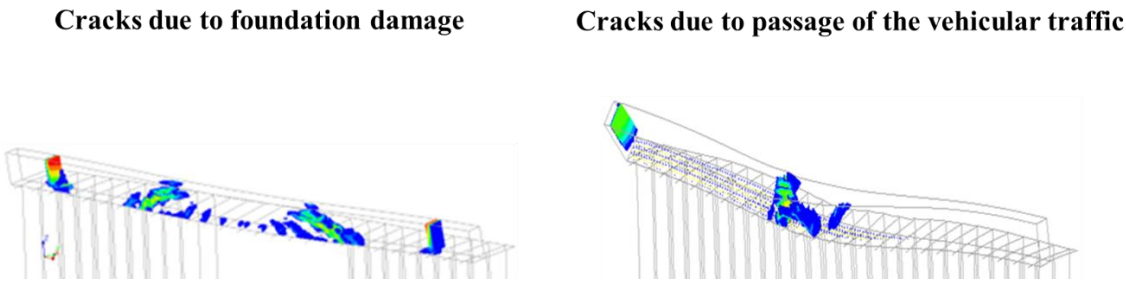

Figure 6: Cracks in a quay wall associated with foundation failure and due to passage of heavy vehicular traffic as observed from numerical simulations reported in [9].

References

[1] Xi, L., and Esposito, R. (2023) A Strategy for Material Characterisation of Multi-wythe Masonry Infrastructure: preliminary study. Report number CM1B20-22-6. Delft University of Technology.

[2] Vermeltfoort, A.T., van de Loo, T.J, and Lamers, H.M. "De druk- en schuifsterkte van metselwerk van de landhoofden van brugnummer 108 te Amsterdam", 20 January 2021, version AV1HML1, TU/e.

[3] Xi, L., and Esposito, R. (2023) Compression test on core extracted from an harbour quay wall. Personal communication 30-3-2023.

[4] NPR 9998:2020 Assessment of structural safety of buildings in case of erection, reconstruction and disapproval - Induced earthquakes - Basis of design, actions and resistances. Nederlands Normalisatie-instituit (NEN).

[5] NPR 9096-1-1: 2010 (Dutch annex to Eurocode 6) Masonry structures - Simple design rules, based on NEN-EN 1996-1-1+C1. Nederlands Normalisatie-instituit (NEN).

[6] Jafari, S., Rots, J. G., & Esposito, R. (2022). A correlation study to support material characterisation of typical Dutch masonry structures. Journal of Building Engineering, 45, 103450.

[7] Gaggero, M. B., & Esposito, R. (2023). Experimental characterisation of flexural bond behaviour in brick masonry. Materials and Structures, 56(3), 62.

[8] EN 1996-1-1+A1 (2013). Eurocode 6 – Design of masonry structures – Part 1-1: General rules for reinforced and unreinforced masonry structures. Nederlands Normalisatie-instituit (NEN).

[9] Sharma, S., Longo, M. and Messali, F. (2023) Tiered based structural assessment of a masonry quay wall in Amsterdam : influence of load redistribution and foundation damage. Report number CM1B20-22-3. Delft University of Technology.

[10] Boscardin D.M. and Cording J.E (1989) Building Response to Excavation-Induced Settlement. Journal of Geotechnical Engineering, 115(1).

[11] De Vent, I.A.E (2011) Prototype of a diagnostic decision support tool for structural damage in masonry, Delft University of Technology.